Publications of the Institute of Geophysics, Polish Academy of Sciences
Geophysical Data Bases, Processing and Instrumentation
vol. 442 (D-77), 2022, pp. 19-40
DOI: 10.25171/InstGeoph_PAS_Publs-2022-023

Nimbostratus and Stratus Cloud Atmospheric Electricity Database and Analysis Methods for the Project "Research Studies on the Electricity of Low-Level Layer Clouds for the Purpose of Developments in Global Atmospheric Circuit Modelling (ELLEC)"

Anna ODZIMEK[1,✉], Piotr BARAŃSKI[1], Marek KUBICKI[1], Danuta JASINKIEWICZ[1*], Jerzy BERLIŃSKI[2*], and Wojciech GAJDA[3]

[1]Institute of Geophysics, Polish Academy of Sciences, Warszawa, Poland

[2]Faculty of Electronics and Information Technology, Warsaw University of Technology, Warszawa, Poland

[3]Institute of Meteorology and Water Management – National Research Institute, Warszawa, Poland

*retired

✉ aodzimek@igf.edu.pl

A b s t r a c t

This paper provides details on meteorological and atmospheric electricity datasets and the methodology of analysis of the atmospheric electric data from the Polish Atmospheric Electricity Observation Network used for the purpose of research studies of the electricity of Nimbostratus and Stratus clouds and their role in the global atmospheric electric circuit.

Keywords: atmospheric electricity, clouds, Nimbostratus, Stratus, global atmospheric electric circuit.

1. INTRODUCTION

The view that not only thunderclouds but also other electrified clouds, such as shower clouds, can generate electricity in the atmosphere has been originally formulated by Wilson (1921), the author of the concept of the global atmospheric electric circuit (GEC). Observations have been indicating that the electrical activity of low-level precipitation-producing clouds, such as Nimbostratus, is manifested by more complex electrical structure and generation of conduction and

© 2022 The Author(s). Published by the Institute of Geophysics, Polish Academy of Sciences.
This is an open access article under the CC BY license 4.0.

precipitation electric currents (Chalmers 1956, 1958; Reiter 1965; Anderson 1966; Magono and Orikasa 1966; Rust and Trapp 2002). Imyanitov et al. particularly observed vertical profiles of the electric field through all kinds of clouds and investigated the profile properties dependent on the cloud genus and thickness, revealing the complex electrical structure of Nimbostratus clouds observed in situ (e.g., Imyanitov and Shifrin 1962; Imyanitov et al. 1974). Reiter (1968, 1972) investigated the electric field and current density under various types of precipitating clouds, including Nimbostratus, in particular during the transition between cloud genera and the absence or presence of precipitation. Based on these results, Odzimek et al. (2010) have constructed a GEC model assuming the low-level Nimbostratus cloud to be a generator in the circuit, in addition to the main convective cloud generator, resulting in a preliminary estimate of the "Nimbostratus" cloud contribution[1] at 20% to the total global current, subsequently revised to about 10% in Odzimek et al. (2018).

In 2011 a scientific project "Research studies on the Electricity of Low-Level Layer Clouds for the purpose of developments in global atmospheric circuit modelling (ELLEC)" has been proposed at the Institute of Geophysics, Polish Academy of Sciences (PAS), subsequently approved and funded by Poland National Science Center (NCN), in order to initiate a comprehensive study on the electricity of low-level layer clouds and their potential role in the global circuit. The project took advantage of the long-term ground-based observations of atmospheric electricity and meteorology, including clouds, at Stanisław Kalinowski Geophysical Observatory of the Institute of Geophysics (IG) PAS in Otwock-Świder, Poland, and, as a supplement, data from two Polish polar stations creating, together with Świder, the Polish Atmospheric Electricity Observation Network (Table 1). Characterised by a large surface area and continuous precipitation (Houze 1993), both Nimbostratus (Ns) and Stratus (St) cloud cases have been investigated. The first results of the project and a framework for future research have been presented in Odzimek et al. (2014), based on data from the years 2005–2013. Over the next two years, the data collection for the project have been extended till 2015, and Odzimek et al. (2018) presented the statistics of the occurrences of Nimbostratus and Stratus in Świder in 2005–2015 and the average values of main atmospheric electricity parameters over 2012–2015.

Table 1

Atmospheric electricity stations contributing to ELLEC project
(Polish Atmospheric Electricity Observation Network)

Observatory name, location, and operating institution	Short name	Period of Ns and St analysis	Geographical coordinates		
			Latitude	Longitude	Altitude
Stanisław Kalinowski Geophysical Observatory, Świder, Poland (IG PAS)	SWI	2005–2015	52.00°N	21.25°E	100 m
Stanisław Siedlecki Polish Polar Station, Hornsund, Svalbard, Norway (IG PAS)	HRN	2005–2015*	77.00°N	15.50°E	20 m
Henryk Arctowski Polish Antarctic Station, King George Island, New Shetland Islands, Antarctica (IBB PAS)	ARC	2013–2015**	62.16°S	58.47°W	20 m

*only 2007–2010 analysed so far in Odzimek et al. (2014),
**not yet fully analysed.

[1]Not to be equated with the electrified shower cloud generator (e.g., Liu et al. 2010).

As the work on the various aspects of electricity of Ns and St clouds based on the archived data is in progress, in this paper we present the details of the cloud and atmospheric electricity database that has been created for the purpose of the project. The structure of the database is the subject of the next section (Section 2), and in another section (Section 3) we describe the details of the atmospheric electricity measurements and methodology behind the analysis performed on the atmospheric electricity data presented in Odzimek et al. (2018), and still applied in the current studies.

2. ATMOSPHERIC ELECTRICITY AND CLOUD DATASET

The ELLEC project database has been so far created mostly from the data gathered at the Geophysical Observatory of the Institute of Geophysics PAS in Świder, Poland (51.15°N, 21.23°E), taking advantage of the meteorological observations contributing to advanced atmospheric electricity monitoring present at the Observatory for several decades (Dziembowska 2009). Atmospheric electricity data from the other Institute – run atmospheric electricity station in Stanisław Siedlecki Polish Polar Station in Hornsund, Svalbard, Norway (77.00°N, 15.50°E) also contributed to the database of cloud cases. In addition, new electric field measurements have been set up and conducted in 2013–2015 at the Institute of Biochemistry and Biophysics (IBB) PAS Henryk Arctowski Polish Antarctic Station in King George Island, New Shetland Islands, Antarctica (62.16°S, 58.47°W), at the same time financed by another NCN grant project (Kubicki et al. 2016). At Hornsund, standard meteorological cloud observations are performed continuously (e.g., Matuszko and Soroka 2013). Therefore, the database has been relatively easily extended by cases from this polar station. An occurrence statistics of Ns and St clouds observed at Hornsund based on the 2007–2010 data has been already presented in Odzimek et al. (2014) and an analysis of the full period is a subject of future publication. Observations at the Arctowski Station were at the time very limited in this respect but some additional observations during and shortly after the project have been requested to be made by the expedition geophysicists conducting atmospheric electricity measurements. The lack of systematic meteorological observations at Arctowski limits the selection of relevant cases from the station, but overall the additional cases provide opportunities for an insight into latitudinal effects in the performed study – since the Świder observations can rather be representative of land and suburban, mid-latitude cases, and the global circuit modelling requires cloud models covering all latitudes.

2.1 Meteorological observations

Meteorological observations are continuously performed at Świder in order to monitor fair weather conditions necessary for the qualification of atmospheric electricity data. The observatory keeps records of standard meteorological parameters, cloud condensation nuclei concentrations, and the intensity and time of onset and ending of precipitation as well as the type and amount of cloud cover (cloudiness). Clouds are observed by visual observations by an observer, with a resolution of 1 hour. The cloud species or varieties are not recorded. More recently all-sky recordings with a colour camera have been used to support the observations, together with a Vaisala CL-31 ceilometer funded by the ELLEC project. The duration of rain, drizzle, and snow and their intensity are estimated from the recordings using a Vaisala Rain Detector DRD11A device, in addition to a standard (Hellmann) rain gauge of the observatory and the SEBA Hydrometrie RG-50 heated rain gauge of the Institute of Meteorology and Water Management – National Research Institute, measuring at Świder usually from spring to autumn. The latter allows estimating the rate of precipitation in mm per time unit. At Hornsund the observations of precipitation have been partly supported by OTT Messtechnik Parsivel weather sensor. Details of the instruments and related observed meteorological variables which are analysed in the project are summarised in Table 2.

Table 2
Summary of supporting meteorological observations

Element	Variables	Observations	Instrumentation	Unit	Range	Station
clouds	cloudiness genus	visual	–	1	0–9	SWI HRN ARC
		technical	all sky camera			SWI
	base altitude	technical	VAISALA ceilometer CL-31	m	0–7600	SWI
precipitation	type and duration	visual	–			SWI HRN ARC
		technical	VAISALA DRD11A Rain Detector OTT Parsivel	min	>= 1 min type recognition supported also by air temperature records	SWI HRN
	intensity	visual	-	1	0–2	SWI HRN ARC
		technical	VAISALA DRD11A rain detector SEBA RG-50 rain gauge OTT Parsivel	arbitrary units 0.1 mm		SWI HRN

2.2 The cloud database

The project's cloud database is based on the observatories' monthly reports of meteorological observations. For the analysis, the information retrieved from the reports on clouds, precipitation, mainly rain, snow, drizzle, granular snow, and other phenomena, e.g., mist, fog, hoar frost, etc., has been stored in binary files whose record variable structure is described in detail in Table 3. Files are named in relation to days of the year in the year-month-day digit format "YYYYMMDD" (YYYY – 4 digits for year, MM – 2 digits for the month of the year, and DD – 2 digits for the day of the month), preceded by the affix "pog" and followed by the station short abbreviation "STN" (SWI for the Świder Observatory, HRN for Hornsund Station, and ARC for Arctowski Station), separated by "_", and with the file extension ".dat". The variables encoded in the binary file created a digital record type consisting of three main fields: the date, clouds record, and phenomena record. The clouds record is also a record type variable of numbers and tables of numbers (integer and double real values), each encoding selected characteristics such as the number of cloud cases which have been observed on the day, the clouds genera, species and varieties, the cloud onset and end time for each genus (resolution of 1 h resulting from the time observations at Świder, 3 h for Hornsund), sky cover (cloudiness) in okta scale (0–8, 9 – sky not visible) by the cloud genus at the time of onset and the end time, and a special flag for the times, encoded by 0 or 1 or 2, meaning: 0 – time from observations at an hour, 1 – approximate hour of onset or end, 2 – time determined only by the climatological

times: n, na, a, p, np (e.g., Chomicz 1962). Atmospheric precipitation and other types of meteorological phenomena have also been encoded in a similar way. The digit (integer) codes for cloud genera, species and variety, and phenomena types are outlined in the Appendix.

As an example we present the record for the day 24 May 2013, when St and Ns cases occurred (Odzimek et al. 2018, Figs. 9–10). Below we show the transcription of the record in symbols denoting variables from Table 3 and expressions used in the written language:

Table 3

Daily cloud dataset encoded into binary file "pog_date(YYYYMMDD)_STN.dat"

Variable	Type	Name*	Values or value range
	record Tpog	pog	record
Structure of daily record Tpog			
date	double	pog.d	date-time value**
clouds record	record Tcl	pog.c	record
phenomena record	record Tph	pog.p	record
Structure of clouds record Tcl			
number of cloud cases	integer	pog.c.count	0-10
table of cloud cases	table of Tcl1	pog.c.tab	indexed table
Structure of cloud record Tcl1			
cloud genus	integer	pog.c.tab[index].typ	see Appendix
cloud species and variety***	set of integer	pog.c.tab[index].gat	see Appendix
cloud time onset	double	pog.c.tab[index].t1	date-time value**
cloud time end	double	pog.c.tab[index].t2	date-time value**
cloud time onset flag	integer	pog.c.tab[index].f1	0, 1, 2
cloud time end flag	integer	pog.c.tab[index].f2	0, 1, 2
cloudiness at the cloud time onset	integer	pog.c.tab[index].c1	0-9
cloudiness at the cloud time end	integer	pog.c.tab[index].c2	0-9
Structure of phenomena record Tph			
number of phenomena	integer	pog.p.count	0-15
table of phenomena cases	table of Tph1	pog.p.tab	indexed table
Structure of phenomenon record Tph1			
phenomenon type	integer	pog.p.tab[index].typ	see Appendix
phenomenon time onset	double	pog.p.tab[index].t1	date-time value**
phenomenon time end	double	pog.p.tab[index].t2	date-time value**
phenomenon time onset flag	integer	pog.p.tab[index].f1	0, 1, 2
phenomenon time end flag	integer	pog.p tab[index].f2	0, 1, 2
phenomenon intensity at its onset	integer	pog.p.tab[index].z1	0-2
phenomenon intensity at its end	integer	pog.p.tab[index].z2	0-2

*suggested name to give an example of the variable reference in the computer code,
**double value such as 0.0 refers to 12/30/1899 12:00 am (as in Delphi programming language),
***only for the dataset of clouds observed at Hornsund (HRN).

Transcription of variable “pog” for 13 May 2013
Date: 2013/05/13
Cloud record:
Number of cloud cases: 2
Cloud 1: St, 2015/04/24 00:00 – 2015/04/24 09:00, flags: (0,0), cloudiness: 8-8
Cloud 2: Ns, 2015/04/24 09:00 – 2015/04/25 00:00, flags: (0,0), cloudiness: 8-8
Phenomena record:
Number of phenomena: 4
Phenomenon 1: Intermittent drizzle, 2013/05/24 01:11 – 2013/05/24 01:14, flags: (0,0), intensity: 0-0
Phenomenon 2: Drizzle, 2013/05/24 01:35 – 2013/05/24 01:56, (0,0), 0-0
Phenomenon 3: Drizzle, 2013/05/24 06:55 – 2013/05/24 09:20, (0,0), 0-0
Phenomenon 4: Rain, 2013/05/24 09:20 – 2013/05/25 00:00, (0,0), 0-2

2.3 Atmospheric electricity database

The atmospheric electricity part of the database includes results of measurements of the atmospheric electricity parameters at a station for the days with cloud events. Data are stored in the text format of a less complicated structure compared to the cloud dataset. The atmospheric electricity parameters measured at Świder are:

- vertical (z) component of the strength of the atmospheric electric field – later in the text called the electric field (measured by two independent sensors, one of which, the collector, measures actually the electric potential gradient),
- vertical (z) component of the strength of the atmospheric electric current density – later in the text called the electric current density,
- positive air conductivity,
- negative air conductivity.

For the purpose of most analyses, the parameters are stored into daily files of 1-minute average values, tabulated, and written in a text format. In one file there are 1440 tabulated values for each atmospheric electricity parameter that is available for the day, preceded by “one minute” introductory text informing about the time resolution and, in the following line, names of the variables in each column. The first column denotes the number of a sample (0..1439). The next columns are atmospheric parameter values, as listed in Table 4. Any missing value is denoted by “*”. The parameters includes atmospheric electric field (at Świder measured by two methods hence two data columns, see next section), atmospheric electric current density, and positive and negative air conductivity as numbers in units as shown in Table 4. The methods of how these parameters are measured and analysed for the purpose of the ELLEC project are described in Section 3. Additionally, in the first half of 2012, short-term measurements of the electric charge on droplets (e.g., Imyanitov 1957) have been performed on several occasions; however, these measurements have been abandoned due to a difficult interpretation of the data from the rarely used instrument.

Sign convention. The convention for the sign of the atmospheric electric field and current density used here is the so-called “fair-weather convention”, i.e., the *z* axis is directed downwards). In fair-weather conditions, the atmospheric electric field is directed downwards and in this convention considered positive. This also means the sign and value of the E_z is the same as that of the electric potential gradient. In regard to the atmospheric electric current density, positive charge transferred downwards (in the direction of fair-weather electric field) becomes positive atmospheric electric current.

Table 4
Daily atmospheric electricity datasets in output text files "date(YYYYMMDD)_STN.dat"*

Variable	Type	Name*	Unit	Range
negative air conductivity	real	cond–	fS/m	0.1–12.0
positive air conductivity	real	cond+	fS/m	0.1–12.0
vertical component of the atmospheric current density	real	J_z	pA/m^2	±20.0
vertical component of the strength of the atmospheric electric field (collector)	integer	Ez(COL)	V/m	±1390 V/m ±4960 V/m (since December 2012)
vertical component of the strength of the atmospheric electric field (field mill)	integer	Ez(FM)	V/m	±1390 V/m ±13.9 kV/m (since May 2013)**

*In the case of data from Hornsund (HRN) or Arctowski (ARC) where only the electric field is measured the columns with remaining variables in the file can be absent,
**Świder (SWI) only.

2.4 Auxiliary radar, satellite, and sounding data

In addition to the ceilometer observations at Świder, we have also obtained for the purpose of the project the meteorological radar, cloud satellite product data, and atmospheric sounding data (Figs. 1 and 2). These are auxiliary data so far used mainly in case studies. The atmospheric sounding data, both in the text and in graphical format such as the skew-T diagrams, have been downloaded from the University of Wyoming web pages at http://weather.uwyo.edu/upperair/sounding.html, for Legionowo (approximately 30 km NNW of Świder). Radar and satellite data have been processed at the Institute of Meteorology and Water Management – National Research Institute (IMWM-NRI) for the purpose of the ELLEC grant project. These datasets cover the selected Ns and St cases from 2012 to mid-2013 (Odzimek et al. 2017a,b).

The radar data come from ground-based meteorological radar observations at Legionowo and include products based on the radar volumetric data for both the classical scan with a range of 250 km, and the Doppler scan with a range of 125 km. As the area of special interest has been defined around the Świder Geophysical Observatory, all products had a range of 100 km (Gajda 2013). Types of generated products include:

- EHT radar echo height (range: 100 km, reflectivity threshold: –5 dBZ);
- EHT radar echo height (range: 100 km, reflectivity threshold: 0 dBZ);
- EHT radar echo height (range: 100 km, reflectivity threshold: 4 dBZ);
- PCAPPI reflectivity at a given altitude (range: 100 km, altitude: 1 km);
- PCAPPI reflectivity at a given altitude (range: 100 km, altitude: 2 km);
- PCAPPI reflectivity at a given altitude (range: 100 km, altitude: 3 km);
- VCUT vertical section for three variants:
  – along the radar beam towards the Świder station (1),
  – north-south direction passing through the Świder station (2),
  – east-west direction passing through the Świder station (3).

The satellite products are based on SEVIRI instrument data from the EUMETSAT Meteosat satellites and present a „cloud type" CT product at 15-min time resolution in the form of graphical information stored in .gif format images (Fig. 2) with an option of access to digital

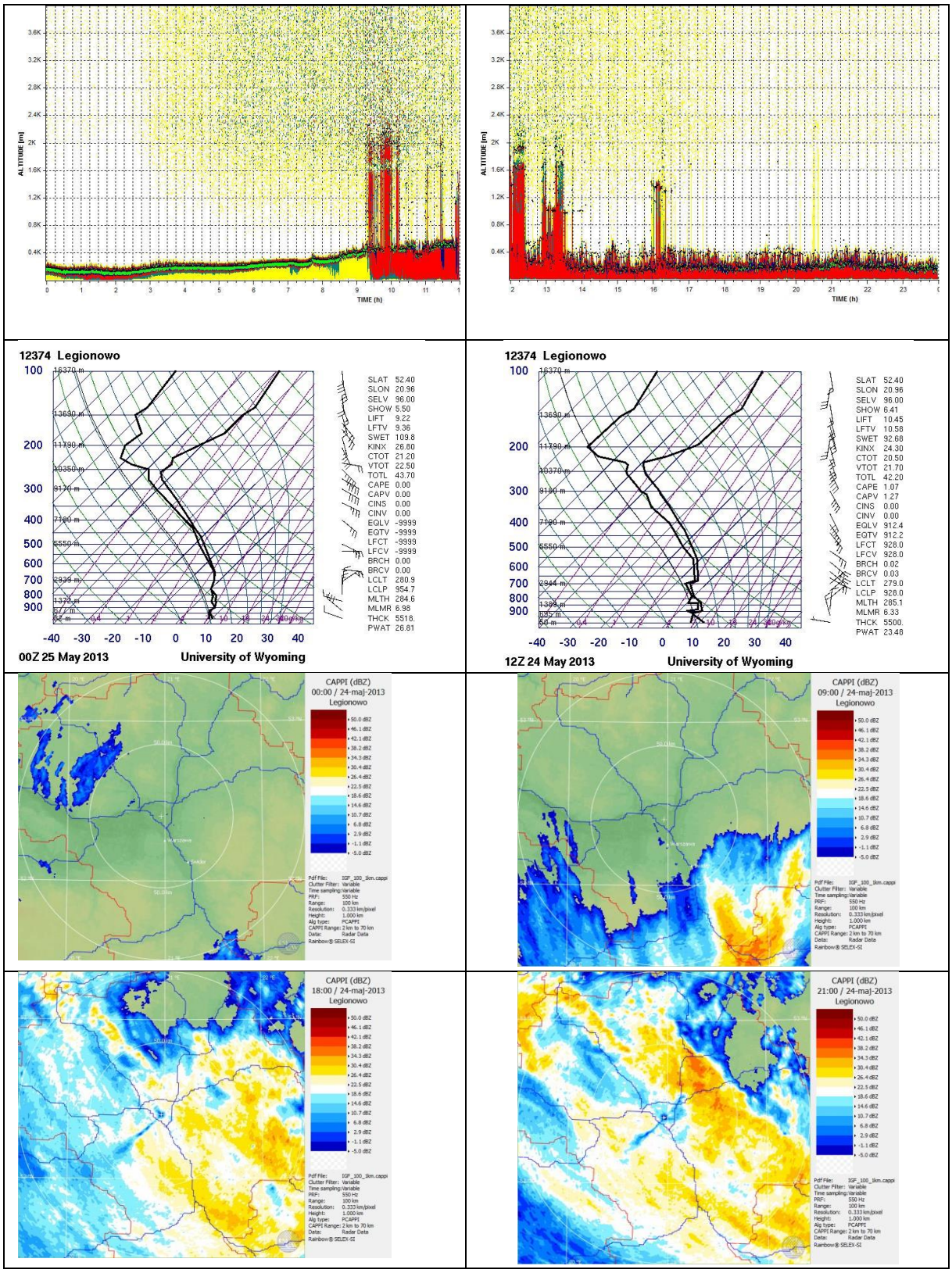

Fig. 1. Selected auxiliary data for 24 May 2013 during an occurrence of St with short drizzle and an Ns cloud with rain: left panel – 00–12 UT, right panel – 12–24 UT, upper panels: ceilometer reflectivity plots from the CL30 ceilometer, middle panels: skew-T diagrams for Legionowo soundings at 0 UT and 12 UT, four bottom panels: Legionowo radar reflectivity (1 km CAPPI) at 00, 09, 12, 21 UT.

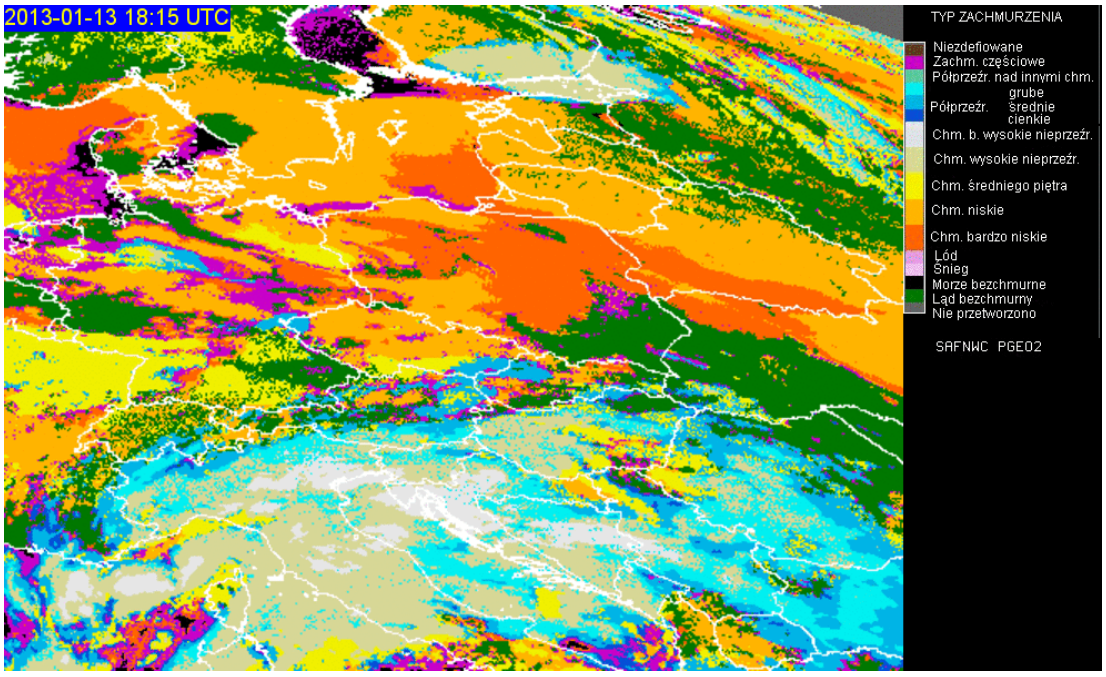

Fig. 2. An example of the EUMETSAT/NWCSAF-IMWM satellite cloud type product from 13 January 2013, 18:15 UTC. The legend on the right side lists possible features (types) of clouds and the cloudiness at the earth surface, as follows: brown – undefined; amaranth – partly cloudy; light green – translucent over other clouds; light-blue, blue, navy – translucent thick, medium, thin; yellow – middle-level clouds; dark yellow – low-level clouds; orange – very low clouds; pink – ice; light pink – snow; black – sea; green – cloudless land; dark grey – not processed.

output in other data formats. The spatial resolution is ~12 km. These data help to confirm the existence of relevant cloud types, and allow calculation of their surface area (Serafin-Rek 2013).

Ceilometer data have been stored in the graphical form as produced from the ceilometer commercial software CL-View, and they present the level of reflectivity and software-calculated values of the cloud base altitude. The images help for example to distinguish a Stratocumulus decay and the formation of Ns or St. During Ns or St with precipitation, the ceilometer allows only the determination of the height of the cloud base. The standard software-produced files which store information on the height of clouds' base in text form have also been preserved and used.

These auxiliary data helped to confirm the existence of low stratiform clouds and precipitation from the clouds at Świder as well as to deliver information on some spatial structure of the precipitation both in the horizontal and vertical direction.

3. ATMOSPHERIC ELECTRICITY MEASUREMENTS AND DATA ANALYSIS

3.1 Measurements

Descriptions of the apparatus used for the measurements of the electric field and conductivity at Świder station have been included in the yearly reports of the results of observations (e.g., Kubicki 2006). Below we enclose the schematic diagrams of the measurement set-up based on the reports.

The electric field strength at Świder station is measured with a radioactive collector method (Witkowski 1902) – these are values annotated in data files by "Ez(COL)", or by a rotating dipole-type field mill – values annotated in the data files by "Ez(FM)". At Hornsund a collector has also been in use but much more reliable measurements are performed simultaneously using

a rotating dipole-type field mill constructed by Berliński et al. (2007). A rotating-dipole field mill of this type has also been used at Arctowski Station in 2013–2015. A schematic diagram of the measurement with the collector (K) is shown in Fig. 3a. The radioactive collector (K) at Świder has a radioactive source of 30 μC activity (Am). The collector is connected to an electrometer constructed in the observatory (e.g., Kubicki 2006), placed inside a metal case at 200 m above the ground level, mounted on a metal pipe. The electrometer has high input resistance $R_{in} = 10^{14}$ Ω, compared with the collector's resistance $R_{coll} = 7 \times 10^{10}$ Ω. Such use of resistances in the circuit eliminates the influence of wind on the electric field measurements. The time constant of the current circuit, including the capacitance of cables, is 7 s.

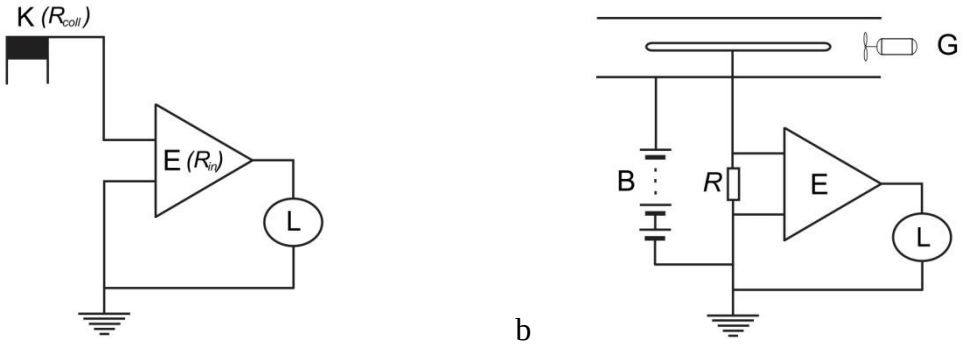

a b

Fig. 3. Schematic diagram for electric field and conductivity measurements at the Geophysical Observatory in Świder (after Kubicki 2006). Apparatus: K – radioactive collector, G – Gerdien tube, L – logger, B – batteries, E – electrometer (of R_{in} input resistance), R_{coll} – collector resistance, R – other resistances (description in the text).

The conductivity is measured with a Gerdien tube (G), also called the Gerdien aspiration condenser (Gerdien 1905), the schematic diagram of which is shown in Fig 3b. It is placed in a hut 1 m above the ground level. One side of the tube is outside of the hut where the air is aspirated. The boundary mobility of the condenser is 2.6×10^{-4} m^2/Vs. The outer electrode is connected to a series of batteries (B). The centre electrode of the tube is connected via a high resistance $R = 100$ GΩ to a Keithley 614 electrometer (E), which measures the current flowing through the resistance R, which is proportional to the conductivity of the air in the tube. The time constant of the circuit is 60 s. There are two separate tubes for the measurements of positive and negative ion polarities.

Analog data are transformed into digital using an Institute-developed data loggers (L) with an analog-to-digital converter and output data stored in .ddf format (e.g., Reda and Neska 2016). A file in a .ddf format is a text file describing the number of channels and time series in each data channel (start time, time shift, resolution, base value, name, units, etc.) and associated files for each channel in binary format. The sampling is usually set to 1 s time resolution. After upload to a data server, the data are numerically averaged to 1-minute values available on a password-protected WWW-based interface for visual inspection in 24-hour data plots, and for download.

Some atmospheric current density measurements from Świder have been available from 2005–2007, in part conducted for the study of fair-weather atmospheric electric convection current, and over 2011–2012 have been restarted as the station measurements of the atmospheric current density J_z. A block diagram of the atmospheric current measurement set-up is shown in Fig. 4. The sensor for the current density measurements is a "Wilson antenna" type (Wilson 1906), i.e., metal (aluminum) flat plate supported by isolators and levelled with the ground. The antenna is of a circular shape of a surface area of 0.5 m^2. The antenna is

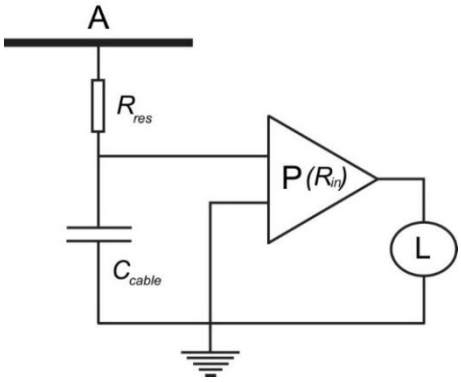

Fig. 4. Schematic diagram of the atmospheric current density measurement at the Geophysical Observatory in Świder. Apparatus: A – metal flat antenna, L – logger, P – picoammeter (of R_{in} input resistance), C_{cable} – cable capacitance, R_{res} – added resistance (description in the text).

connected to a Keithley 867 picoammeter (P) in series with a 10^{11} Ω resistor R_{res}. A cable from the antenna to the picoammeter in the building (300 m) has an estimated capacitance C_{cable} = 300 pF (1000 pF in other configurations used before 2012). The role of the $R_{res} = 10^{11}$ Ω resistance is to limit the amplitude of the displacement current received by the antenna. A numerical simulation of the schematics with the OrCAD PSpice A/D, an electronic circuit simulation software, has indicated that the average amplitude of the input signal decreased approximately to 0.8 of the input level. Therefore, the output values of the current have been multiplied by 1/0.8 = 1.25.

In general, such antenna detects all components of the atmospheric Maxwell current which includes conduction, precipitation, convection, corona, lightning, and the displacement current (e.g., MacGorman and Rust 1998, Chapter 1). In regard to the conduction component received by the antenna, it is important to take into account that it measures only part of the conduction current, that is carried by the ions which are able to reach the antenna in the direction of the electric field – this means they are the ions of an electric charge sign the same as the sign of the electric field. In the case of other components where electric charge is transferred gravitationally or mechanically, components of both signs are received.

3.2 Data analysis

Our study of the electricity of clouds from ground-level atmospheric electricity measurements is based on the analysis of the electric field, conductivity, and current density components which participate in the charge transfer in the air between the cloud and the ground. A similar approach was used by, e.g., Aspinall (1969). Because the considered cloud data span a larger period of time we have used only the electric field data measured by the radioactive collector method, i.e., the E_z values from the Ez(COL) records. As mentioned, the total Maxwell current density in the atmosphere consists of several components characteristic of the way of charge transfer in the process, e.g., conduction, lightning, or corona. In case of Stratus and isolated Nimbostratus, i.e., not in connection with a thunderstorm system such as the mesoscale convective system (Michnowski et al. 1987; Houze 1993), we assume that lightning, and related to it lightning current density component, is usually absent (this can also be confirmed by meteorological observations and is monitored in the electric field signal). We also neglect corona current density effects, taking into account that we work in a sufficiently low electric field range. The remaining current density components of the Maxwell current density J_M (Eq. 1) that are required to be taken into account are:

- vertical conduction field component J_E (in other publications denoted J_C), according to Ohm law equal to the product of air conductivity and the electric field strength E_z (Eq. 2);

- precipitation or convection current J_{PC} (in general representing the charge transfer by various mechanical processes, and not by conduction);
- the displacement current J_D, theoretically expressed by the time derivative of the electric field multiplied by the dielectric permittivity of free space $\varepsilon_0 = 8.854 \times 10^{12}$ F/m (Eq. 3).

$$J_M = J_E + J_{PC} + J_D = J_T \ , \tag{1}$$

$$J_E = (\lambda_+ + \lambda_-)\, E_z = \lambda\, E_z \ , \tag{2}$$

$$J_D = \varepsilon_0\, \partial E_z / \partial t \ , \tag{3}$$

$$J_T = J_E + J_{PC} \ . \tag{4}$$

After separating the displacement current density from the Maxwell current we obtain the current density component J_T (total) (Eq. 4), referring to the current density due to the total charge transfer under the cloud to the ground (Chalmers 1958). The total current J_T takes into account the charge transferred by both the conduction and precipitation or convection. These three current components, J_E, J_{PC}, and their sum J_T, are the major parameters we study. In the next paragraph, we describe how we determine these current density components from the ground-based atmospheric electricity measurements at Świder. The method has already been used in Odzimek et al. (2018) and would also be applied in future work.

In the analysis of the atmospheric electricity, we use 5-minute average values of the electric parameters which we calculate from already averaged 1-min text atmospheric electricity data. We therefore can rewrite the Eqs. 1–4 for the average values:

$$\langle J_M \rangle = \langle J_E \rangle + \langle J_{PC} \rangle + \langle J_D \rangle = \langle J_T \rangle + \langle J_D \rangle \ , \tag{5}$$

$$\langle J_E \rangle = \langle \lambda\, E_z \rangle \ , \tag{6}$$

$$\langle J_D \rangle = \langle \varepsilon_0\, \partial E_z / \partial t \rangle \cong 0 \ , \tag{7}$$

$$\langle J_T \rangle = \langle J_E \rangle + \langle J_{PC} \rangle \ . \tag{8}$$

Taking into account, that the displacement current component is reduced both by the current measurement set-up and by the time averaging of the 1-min data, we further assume that in the 5-min averages this component is negligible.

Conduction current J_E

The conduction current density J_E is determined from the Ohm law that relates the conduction current density to the total conductivity λ (the sum of the unipolar conductivities λ_+ and λ_-) multiplied by the electric field, E_z (Eq. 2). According to this definition, the sign of the component is in agreement with the sign convention for the electric field (transport of positive charge downwards is positive).

Precipitation-convection current J_{PC}

As indicated above, in theory, by subtracting from the Maxwell current density the values of the two other components, i.e., the displacement current J_D and conduction current J_E, both possible to be determined from the direct measurements of the electric field, E_z, and the conductivity, λ, we are able to evaluate the precipitation component J_{PC}. When measuring the Maxwell current density by the Wilson antenna, one should take into account in the subtraction only the polarity which agrees with the direction of the electric field, $J_{\lambda(E)}$:

$$J_{PC} = J_z - J_{\lambda(E)} \ , \tag{9}$$

$$J_{\lambda(E)} = \lambda_+ E_z \quad \text{if} \quad E_z > 0 \ , \tag{10}$$

$$J_{\lambda(E)} = \lambda_- E_z \quad \text{if} \quad E_z < 0 \ , \tag{11}$$

where J_z is the measured Maxwell current density, $J_{\lambda(E)}$ is the conduction current component related to the electric field and unipolar conductivity in agreement with the sign of the electric field, i.e., $J_{\lambda(E)} = \lambda_+ E_z$ when $E_z > 0$ or $J_{\lambda(E)} = \lambda_- E_z$ when $E_z < 0$.

The final set of equations for the determination of the current density components from measurements is:

$$<J_E> = <\lambda E_z> = < (\lambda_+ + \lambda_-) E_z> \ , \tag{12}$$

$$<J_{PC}> = <J_z> - <J_{\lambda(E)}> \ , \tag{13}$$

$$<J_T> = <J_E> + <J_{PC}> \ . \tag{14}$$

The above scheme of calculations has been used with the measurements collected for the purpose of the ELLEC project over 2012–2015. However, for a short period of time the measurements of the current density were performed with a screened antenna. The aim of this experiment was to measure the precipitation-convection current density J_{PC} directly. Such a measurement was arranged by covering the Maxwell current density sensor by a grounded cuboid metal mesh, made of 2 mm metal wire, mesh size 4 cm by 4 cm, with four rectangular sides and a square surface area of 1 m^2 placed 40 cm above the antenna level (Odzimek et al. 2018, Fig. 4). We have temporarily conducted such measurements over approximately one month in the spring of 2013 (May/June). The antenna surface area covered by the mesh was ≅4.4% of its total surface area. The screened antenna, in an ideal situation, should not receive the conduction current and other field-dependent current components, thus detecting only the current of the charge transferred by precipitation or convection. Monitoring the sign and value of J_{PC} component gives a possibility to evaluate the total amount of electric charge deposited on the ground by precipitation particles descending from different types of electrified clouds or the charged particles carried by convection. Although in the past other methods of measurement of the precipitation current have been used (Imyanitov 1957), the method of measurements using an antenna has also been in use (e.g., Ramsay and Chalmers 1960; Aspinall 1969). Unfortunately, it was impossible at the time of the project to conduct simultaneous measurements with exposed and screened antenna. Such an experiment would be very valuable for comparison and validation of results.

In the measurement set-up with the screened antenna, we equate the measured current J_z with the precipitation-convection current J_{PC}, and the calculations scheme for this period becomes as follows:

$$<J_z> = <J_{PC}> \ , \tag{15}$$

$$<J_E> = <\lambda E_z> = < (\lambda_+ + \lambda_-) E_z> \ , \tag{16}$$

$$<J_{T>} = <J_E> + <J_{PC}> \ . \tag{17}$$

Below we show some examples of the time series of the current components measured and derived in the way described above. The first is an example of a rain episode from 3 October 2012 in Fig. 5, and the second with a snowfall on 20 January 2015 in Fig. 6. These two examples are characterised by relatively small amplitudes of the electric field, $|E_z| < 1000$ V/m, and small variations of the conductivities. The other case with drizzle and rain is from 24 May 2013. In this case, the current antenna was screened. This is a case with rather high (negative) values of the electric field, as is the case with another snowfall event on 27 October 2012 (mostly positive

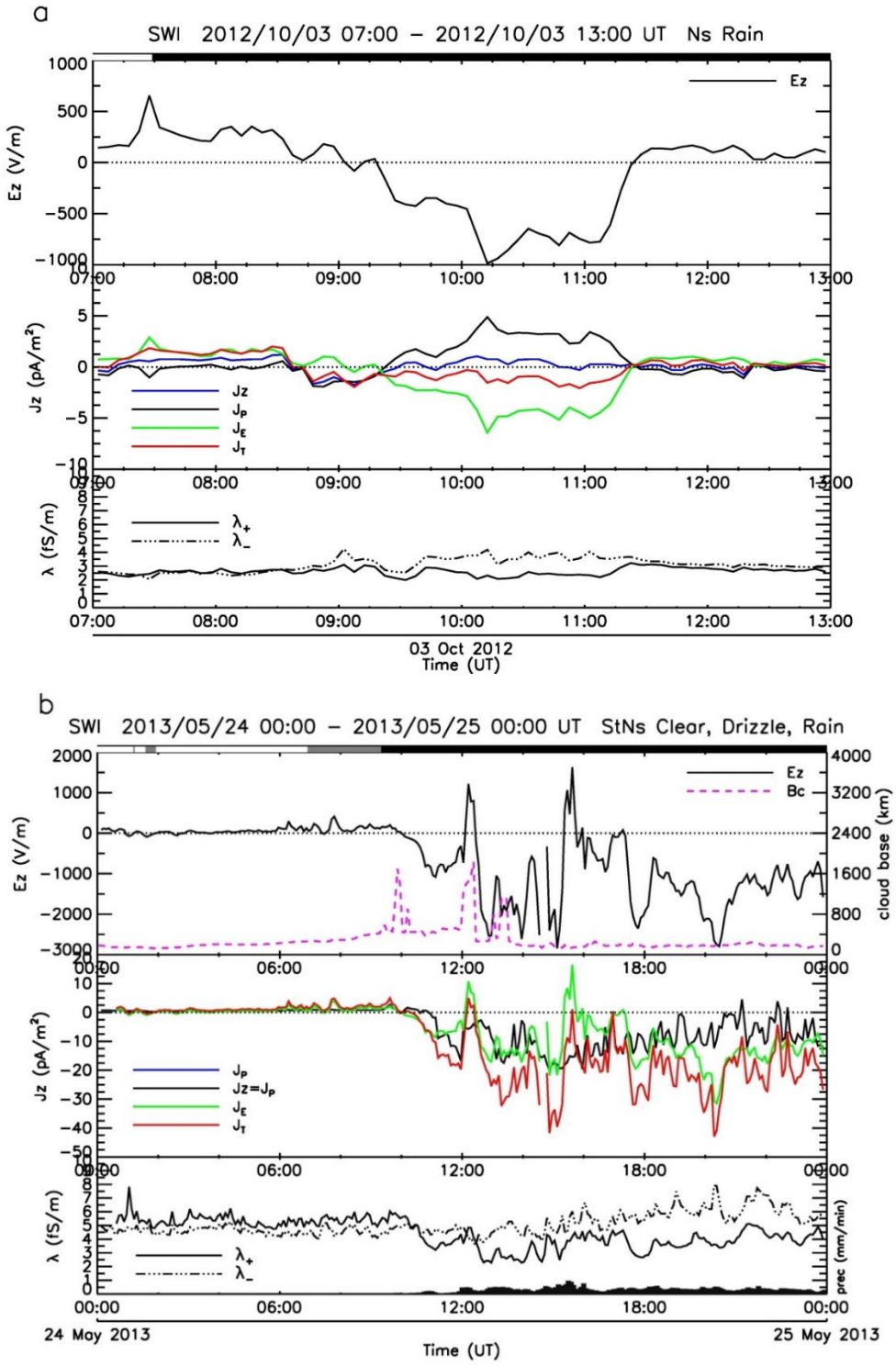

Fig. 5. Time series of 5-min average values of the electric field, current density, and air conductivity under Stratus and raining Nimbostratus clouds at Świder on: (a) 3 October 2013, 00:00–13:00 UT, Ns; (b) 24–25 May 2013, 00:00–00:00 UT, St till ~9:00 UT, then Ns. Upper panel – the electric field (E_z), cloud base (B_c) as determined by the ceilometer – when available; middle panel – variations of the measured and calculated components of vertical ground-level current density, i.e., the measured J_z component, precipitation current density J_{PC}, conduction current density J_E, and total current density J_T, bottom panel – positive and negative air conductivity. In cases (a) J_{PC} was calculated and in case (b) measured. Periods of precipitation are indicated by the coloured stripes above the upper panel: black for rain, and grey for periods of drizzle. In the bottom panel of (b) plotted are 5-min averaged G-50 rain gauge precipitation rates.

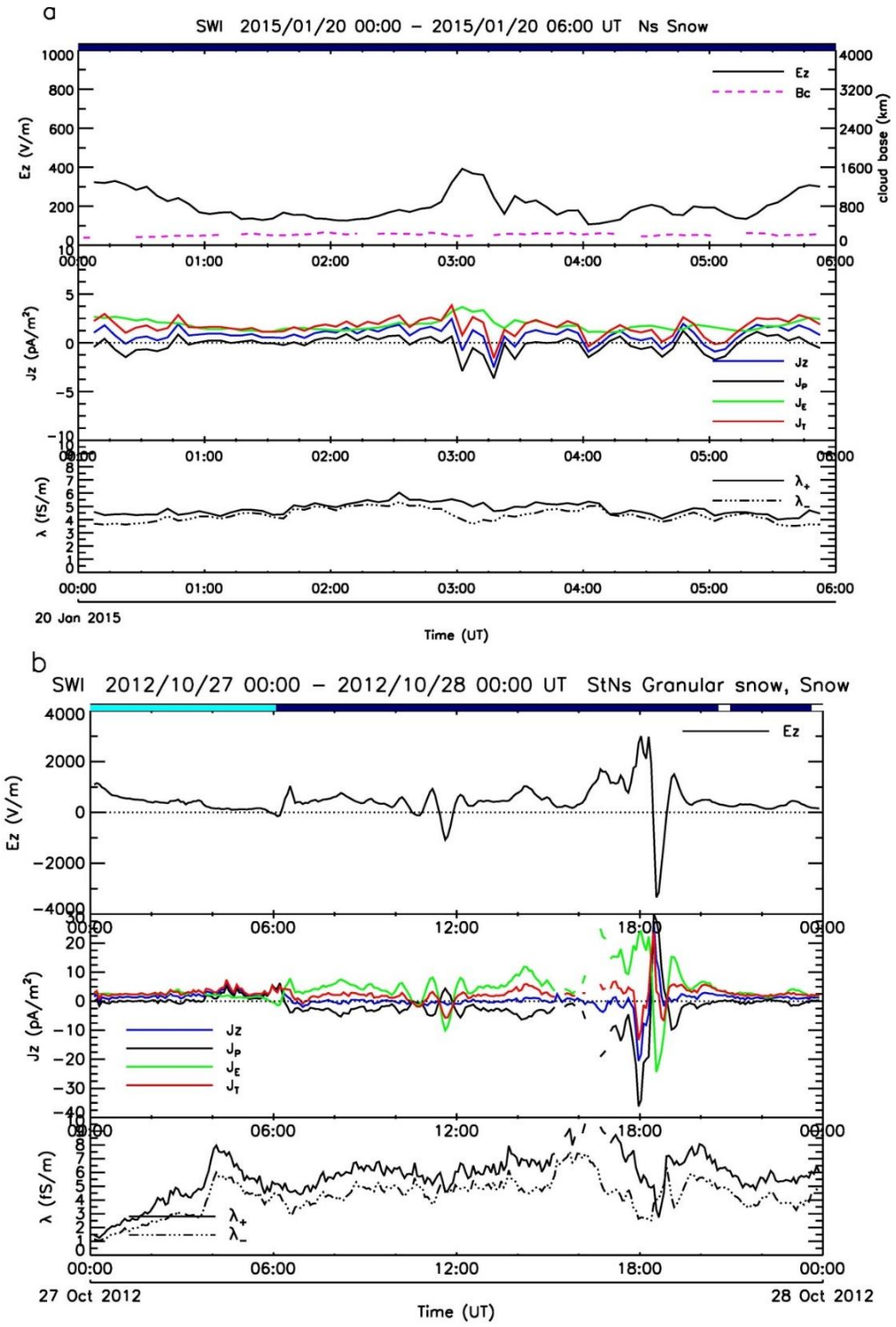

Fig. 6. Time series of 5-min average values of the electric field, current density, and air conductivity under snowing Stratus and Nimbostratus clouds at Świder on: (a) 20 January 2015, 00:00–06:00 UT, Ns; (b) 27–28 October 2012, 00:00–00:00 UT, St followed by Ns at ~6:00 UT. Upper panel – electric field (E_z), and cloud base (B_c) as determined by the ceilometer – when available; middle panel – time variations of the measured and calculated components of vertical ground-level current density, i.e., the measured J_z component, precipitation current density J_{PC}, conduction current density J_E, and total current density J_T, bottom panel – positive and negative air conductivity. In both cases, (a) and (b), J_{PC} component was calculated. Periods of precipitation are indicated by the coloured stripes above the upper panel: navy for snow, and turquoise for periods of granular snow.

but not so stable, e.g., Reiter has determined the stability conditions by the number of the field reversals per hour). The electric field during stable rainfall almost always gets and remains negative, as is the case in the first example, while during snowfall the field stays mostly positive (see, e.g., Odzimek et al. 2018). Note that the total current J_T during snow is mostly positive (i.e., downward, as in fair weather) and during rain it can become negative (i.e., upward). This has consequences for the charging of the global atmospheric electric circuit which we investigated in other publications.

Error analysis

The calculated values of the current density components have inevitably large errors since in addition to the measurement error (5–10% of the value, depending on the variable) there are large deviations related to averaging the values which can strongly vary in time. In such a case, often the median value and interquartile range are used as representative of average values and its error but we rather use an average mean value which seems more appropriate and also used by other researchers. The standard deviation of the mean is always relatively high due to the large time variability of the detected signals (up to 55%). In Table 5 we give a summary of the percentage errors.

Table 5

Summary of percentage errors of the electric measurements and calculated average mean values

Variable		Measurement error	Averages	Standard deviation of 5-min average value
E_z	100 V/m	5%	$<E_z>$	50%
λ_+, λ_-	5 fS/m	10%	$<\lambda_+>$	20%
J_z	5 pA/m^2	10%	$<J_z>$	50%

4. DATA AVAILABILITY

Datasets described in the paper are at present available on demand from the ELLEC project principal investigator Anna Odzimek (aodzimek@igf.edu.pl). The electric and cloud data will be submitted to the Institute of Geophysics PAS Data Portal at ELLEC-dedicated website https://dataportal.igf.edu.pl/group/ellec. Links to already created open-access datasets on Ns and St events from Świder, originally submitted to RePOD ICM UW repository, were added in 2021. More data and metadata of relevant datasets will be subsequently added, however, the binary files of cloud records are to be converted to open file formats and similar data structures. In regard to the ELLEC radar and satellite data, there are terms and conditions of reuse for other purposes as determined by the IMWM-NRI – IG PAS agreement concluded with the data order; more information can be obtained from the PI.

Figure 7 summarises the availability of each kind of data of the project, for the dates with cases of Ns and St clouds at Świder – 711 of individual Ns, St, or mixed St-Ns cases-dates of duration 4113 hours in total for years 2012–2015. These are the data that since mid-2012 could potentially be used for the full analysis that is presented in Section 3 (data from Hornsund and Arctowski do not present this opportunity since only the electric field is recorded). The existence of relevant data is indicated by the grey-coloured stripes: starting from the bottom: the described above "pog" cloud information files (Table 1), i.e., the basic 100%, auxiliary data files for the atmospheric sounding profiles from Legionowo at the term closest to the beginning of a case (00 or 12 UT) – usually of high availability where the atmospheric soundings are regular, the set of electric data (Table 3) for at least 50% duration of the case, necessary to

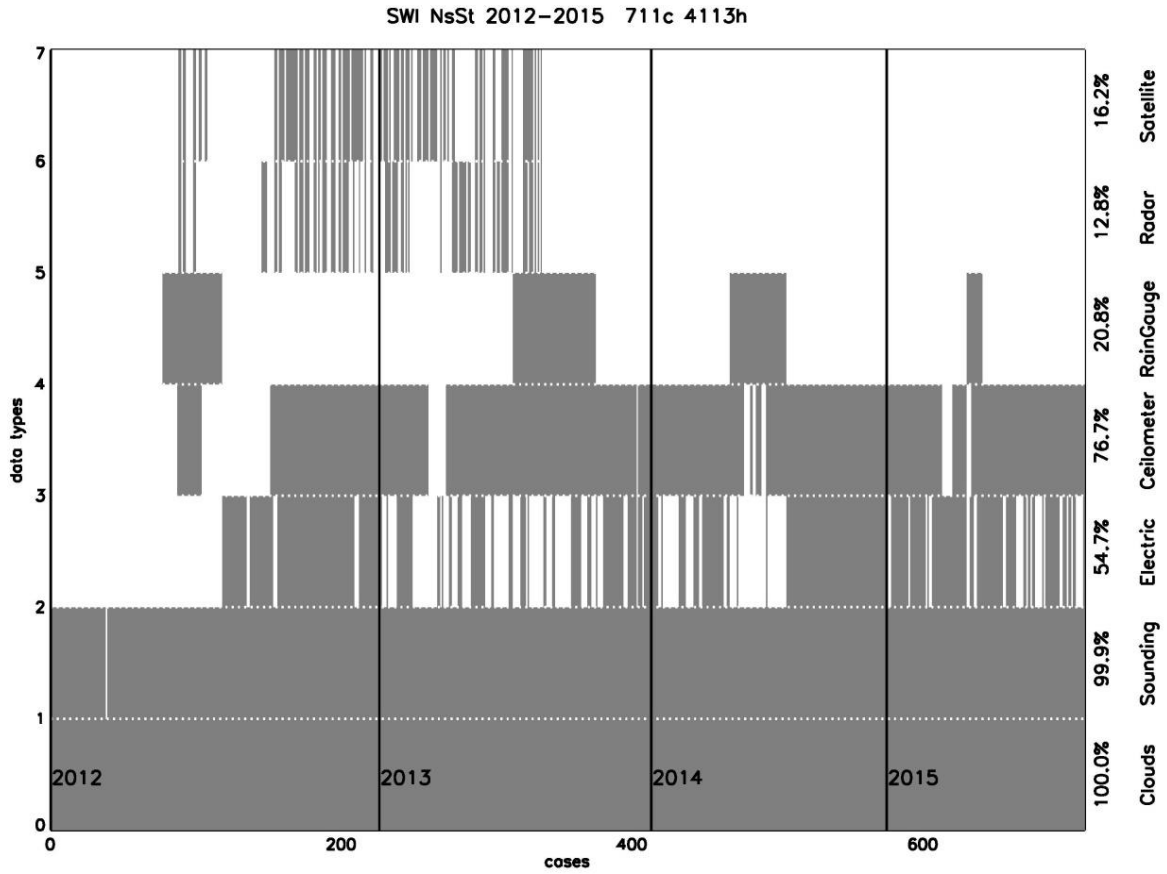

Fig. 7. Availability of the datasets relevant to the project and the identified St-Ns cases at Świder Station for the period 2012–2015. Here the cases are sorted by date, i.e., cases spanned over two or more days are split into several cases encoded in the date-related "pog" files (bottom row – clouds).

derive the total current (Eqs. 14 and 17), ceilometer recordings, rain gauge recordings, radar data, and satellite data. The availability of the electrical data is limited mainly by the absence of technically correct recordings of the current density, and, to a much less degree, of conductivity and the electric field. The availability of the ceilometer recordings is mainly limited by technical breaks in operation at the observatory. The technical breaks and failures decreased the usefulness of the data for the project aims significantly. For example, the full electric set data are usable for ~55% of cases. The rain gauge recordings allowing calculations of the precipitation rates are available mainly in warm seasons, and together with a full electric set the data are available for only ~30 cases, i.e., ~4%. The satellite and Legionowo radar datasets have been obtained for the identified then St and Ns cases at the end of the ELLEC grant project in late spring 2013, and do not cover the later cases. Nevertheless, the data and knowledge gathered during the project provide opportunities for extended research. The current and future studies concern the electricity of precipitation, and further investigation on the electrical structure of clouds and their role in the global circuit.

Acknowledgments. This work was financed by the Institute of Geophysics of the Polish Academy of Sciences with a subsidy from Poland's Ministry of Education and Science.

The scientific research and creation of the database have been supported by Polish National Science Centre grant NCN-2011/01/B/ST10/07188 (2011–2013) and grants of Poland's Ministry of Science and Higher Education (now Ministry of Education and Science) for the statutory activities of the Institute of Geophysics, Polish Academy of Sciences, Nos. 3841/E-

41/S/2014, 3841/E-41/S/2015, 3841/E-41/S/2016, 3841/E-41/S/2017, and 3841/E-41/S/2018. Observations at Hornsund and Arctowski Station have been particularly supported by the Polish National Science Centre grant NCN-2011/01/B/ST10/07118 (2011–2014).

Anna Odzimek expresses gratitude to Andrzej Kułak of AGH University of Technology for very helpful discussions on the atmospheric current measurement methods and the performance of the atmospheric current measurement apparatus at Świder. Anna Odzimek also thanks Magdalena Mielniczek for her voluntary help in uploading Legionowo atmospheric sounding data available from the University of Wyoming atmospheric sounding data website.

Appendix

INTEGER CODES FOR CLOUD GENERA, SPECIES AND VARIETY, AND PHENOMENA TYPES

Cloud genera

Code	Cloud genus
1	Ci
2	Cc
3	Cu
4	Cb
5	As
6	Ac
7	Cs
8	Sc
9	Ns
10	St

Cloud species and varieties

Code	Species or variety
0	None
1	Fibratus
2	Uncinus
3	Spissatus
4	Castellanus
5	Intortus
6	Vertebratus
7	Radiatus
8	Duplicatus
9	Mamma
10	Floccus
11	Stratiformis
12	Lenticularis
13	Undulatus

14	Lacunosus
15	Virga
16	Fractus
17	Humilis
18	Mediocris
19	Congestus
20	Praecipitatio
21	Arcus
22	Tuba
23	Pileus
24	Velum
25	Pannus
26	Calvus
27	Capillatus
28	Incus
29	Translucidus
30	Nebulosus
31	Opacus
32	Perlucidus

Phenomena

Code	Phenomenon
1	Rain
2	Intermittent rain
3	Drizzle
4	Intermittent drizzle
5	Freezing rain
6	Freezing drizzle
7	Snow
8	Intermittent snow
9	Granular snow
10	Sleet
11	Intermittent sleet
12	Intermittent granular snow
13	Hail
14	Soft hail
15	Small hail
16	Grains of ice
17	Ice needles
18	Snow-storm
19	Drifting snow near the ground
20	Drifting snow high up
21	Hoar frost
22	Soft rime

23	Glazed frost
24	Glazed frost on the ground
25	Fog
26	Ground fog
27	Mist
28	Ground mist
29	Ice mist
30	Layer mist
31	Haze
32	Dust haze
33	Dew
34	White frost
35	Water dust
36	Thunderstorm
37	Distant thunderstorm
38	Lightning
39	Tornado
40	Solar halo
41	Lunar halo
42	Rainbow
43	Aurora
44	Drizzle and rain
45	Intermittent drizzle and rain
46	Wind gusts
47	Freezing drizzle and snow
48	Intermittent freezing drizzle and snow
49	Intermittent freezing rain
50	Intermittent freezing drizzle
51	Solar corona
52	Lunar corona

References

Anderson, R.V. (1966), Measurements of total current density above active snowstorms, *J. Atmos. Terr. Phys.* **28**, 8, 789-790, DOI: 10.1016/0021-9169(66)90026-2.

Aspinall, W.P. (1969), Atmospheric Electric Charge Transfer in Precipitation and Associated Synoptic Conditions, PhD Thesis, Durham University.

Berlinski, J., G. Pankanin, and M. Kubicki (2007), Large scale monitoring of troposphere electric field, **In:** *Proc. 13th International Conference on Atmospheric Electricity, 13–17 August 2007, Beijing, China*, Vol. I, 124–126.

Chalmers, J.A. (1956), The vertical electric current during continuous rain and snow, *J. Atmos. Terr. Phys*. **9**, 5–6, 311–321, DOI: 10.1016/0021-9169(56)90149-0.

Chalmers, J.A. (1958), The electricity of Nimbo-Stratus clouds. **In:** L.G. Smith (ed.), Recent Advances in Atmospheric Electricity, Proceedings of the 2nd Conference on Atmospheric Electricity, New Hampshire, 20–23 May 1958, Pergamon Press, New York, 309–315.

Chomicz, W. (ed.) (1962), *Instrukcja dla Stacji Meteorologicznych*, Państwowy Instytut Hydrologiczno-Meteorologiczny. Seria A, Instrukcje i Podręczniki, Wydawnictwa Komunikacji i Łączności, Warszawa (in Polish).

Dziembowska, A. (2009), Eighty years of fair-weather atmospheric electricity monitoring in Poland, *Publs. Inst. Geoph. PAS* **D-73 (412)**, 9–14.

Gajda, W. (2013), Opracowanie danych radarowych poświęcone elektryczności chmur Nimbostratus i Stratus, digital document prepared for the purpose of ELLEC project, 15 pp. (in Polish).

Gerdien, H. (1905), Demonstration eines Apparates zur absoluten Messung der elektrischen Leitfähigkeit der Luft, *Phys. Z.* **6**, 800–801 (in German).

Houze, R.A., Jr. (1993), *Cloud Dynamics*, Academic Press Inc., New York.

Imyanitov, I.M. (1957), *Instruments and Techniques for Investigating the Electricity of the Atmosphere* [Pribory i metody dlya izucheniya elektrichestva atmosfery], Gostekhizdat, Moscow (in Russian).

Imyanitov, I.M., and K.S. Shifrin (1962), Present state of research on atmospheric electricity, *Sov. Phys. Usp.* **5**, 2, 292–322, DOI: 10.1070/PU1962v005n02ABEH003413.

Imyanitov, I.M., Ye.V. Chubarina, and Ya.M. Shvarts (1974), *Cloud Electricity* [Elektryczność Chmur], Państwowe Wydawnictwo Naukowe, Warszawa, 139 pp. (in Polish).

Kubicki, M., (2006), Results of Atmospheric Electricity and Meteorological Observations, S. Kalinowski Geophysical Observatory at Świder, 2005, *Publs. Inst. Geoph. PAS* **D-71 (391)**.

Kubicki, M., A. Odzimek, M. Neska, J. Berliński, and S. Michnowski (2016), First measurements of the Earth's electric field at the Arctowski Antarctic Station, King George Island, by the new Polish atmospheric electricity observation network, *Acta Geophys.* **64**, 6, 2630–2649, DOI: 10.1515/acgeo-2016-0096.

Liu, C., E.R. Williams, E.J. Zipser, and G. Burns (2010), Diurnal variations of global thunderstorms and electrified shower clouds and their contribution to the global electrical circuit, *J. Atmos. Sci.* **67**, 2, 309–323, DOI: 10.1175/2009JAS3248.1.

MacGorman, D., and W.D. Rust (1998), *The Electrical Nature of Storms*, Oxford University Press, New York, 422 pp.

Magono, C., and K. Orikasa (1966), On the disturbance of surface electric field caused by snowfall, *J. Meteorol. Soc. Japan Ser. II*, **44**, 260–278, DOI: 10.2151/jmsj1965.44.5_260.

Matuszko, D., and J. Soroka (2013*), Zachmurzenie Spitsbergenu na Podstawie Obserwacji w Polskiej Stacji Polarnej w Hornsundzie. Cloudiness over Spitsbergen Based on Observations Made at the Polish Polar Station in Hornsund*, Instytut Geografii i Gospodarki Przestrzennej UJ, Kraków, 96 pp.

Michnowski, S., S. Israelsson, J. Parfiniewicz, M.A. Enaytollah, and E. Pisler (1987), A case of thunderstorm system development inferred from lightning distribution. **In:** *Publs. Inst. Geoph. PAS* **D-26 (198)**, 3–57.

Odzimek, A., M. Lester, and M. Kubicki (2010), EGATEC: A new high-resolution engineering model of the global atmospheric electric circuit—Currents in the lower atmosphere, *J. Geophys. Res.: Atmos.* **115**, D18, D18207, DOI: 10.1029/2009JD013341.

Odzimek, A., M. Kubicki, and P. Barański (2014), Ground-level atmospheric electricity under low-level stratiform clouds. **In:** *Proc. 15th International Conference on Atmospheric Electricity, 15-20 June 2014, Norman, USA,* 7 pp.

Odzimek, A., M. Kubicki, P. Barański, and D. Jasinkiewicz (2017a), Nimbostratus cloud cases at Geophysical Observatory IG PAS in Świder in 2005–2015, RepOD, V1, DOI: 10.18150/repod.2362097.

Odzimek, A., M. Kubicki, P. Barański, and D. Jasinkiewicz (2017b), Stratus cloud cases at Geophysical Observatory IG PAS in Świder in 2005–2015, RepOD, V1, DOI: 10.18150/repod.8954639.

Odzimek, A., P. Barański, M. Kubicki, and D. Jasinkiewicz (2018), Electrical signatures of Nimbostratus and Stratus clouds in ground-level vertical atmospheric electric field and current density at mid-latitude station Świder, Poland, *Atmos. Res.* **209**, 188–203, DOI: 10.1016/j.atmosres.2018.03.018.

Ramsay, M.W., and J.A. Chalmers (1960), Measurements on the electricity of precipitation, *Q. J. Roy. Meteorol. Soc.* **86**, 370, 530–539, DOI: 10.1002/qj.49708637010.

Reda, J., and M. Neska (2016), The One Second data collection system in Polish geomagnetic observatories, *J. Ind. Geophys. Union, Sp. Vol.* **2**, 62–66.

Reiter, R. (1965), Precipitation and cloud electricity, *Q. J. Roy. Meteorol. Soc.* **91**, 387, 60–72, DOI: 10.1002/qj.49709138709.

Reiter, R. (1968), Results of investigation on precipitation and cloud electricity based on 15 years of observation, *Arch. Met. Geoph. Biokl. Ser. A* **17**, 17–29, DOI: 10.1007/BF02250790.

Reiter, R. (1972), Contribution to the problem of precipitation electricity, *Arch. Met. Geoph. Biokl. Ser. A* **21**, 247–272, DOI: 10.1007/BF02247975.

Rust, W.D., and R.J. Trapp (2002), Initial balloon soundings of the electric field in winter nimbostratus clouds in the USA, *Geophys. Res. Lett.* **29**, 20, 20-1–20-4, DOI: 10.1029/2002GL015278.

Serafin-Rek, D. (2013), Opis SAFNWC-Seviri, digital document prepared for the purpose of ELLEC project, 3 pp.

Wilson, C.T.R. (1906), On the measurement of the earth-air current and on the origin of atmospheric electricity, *Proc. Cambridge Philos. Soc.* **13**, 6, 363–382.

Wilson, C.T.R. (1921), Investigations on lightning discharges and on the electric field of thunderstorms, *Phil. Trans. Roy. Soc. London A* **211**, 73–115, DOI: 10.1098/rsta.1921.0003.

Witkowski, M.-A. (1902), Note sur l'électricité atmosphérique á Zakopane dans les Tatras [Spostrzeżenia nad elektrycznością atmosferyczną w Zakopanem], *Bull. Int. Acad. Sci. Cracovie* **1**, 7-10.

Received 16 September 2022
Received in revised form 30 December 2022
Accepted 31 December 2022